Journal of Catalysis **205,** 32–43 (2002)
doi:10.1006/jcat.2001.3368, available online at http://www.idealibrary.com on IDEAL®

Catalytic Partial Oxidation of Ethane to Acetic Acid over $Mo_1V_{0.25}Nb_{0.12}Pd_{0.0005}O_x$

II. Kinetic Modelling

David Linke,* Dorit Wolf,* Manfred Baerns,*,[1] Sabine Zeyβ,† and Uwe Dingerdissen†

*Institute for Applied Chemistry Berlin-Adlershof, Richard-Willstätter-Str. 12, D-12489 Berlin, Germany; and †Aventis Research and Technologies GmbH & Co KG, D-65926 Frankfurt a.M., Germany

Received December 6, 2000; revised July 12, 2001; accepted August 1, 2001

DEDICATED TO PROFESSOR ALBERT RENKEN ON THE OCCASION OF HIS 60TH BIRTHDAY

The kinetics of the oxidation of ethane to acetic acid was modelled based on experimental data obtained in a fixed-bed reactor using the title catalyst at temperatures between 500 and 580 K and elevated pressures from 1.3 to 2.8 MPa. The kinetic data were fitted. Two different models taking into account surface processes such as catalyst reduction by ethane or ethylene and reoxidation by oxygen and surface hydroxylation were suggested; the models were discriminated on the basis of experimental data. For the superior kinetic model two different catalytic centres were assumed, i.e., one for the oxidative dehydrogenation of ethane and one for the heterogeneous Wacker oxidation of ethylene to acetic acid. The activity of the Wacker centre strongly depends on the presence of water. The analysis of the kinetic results leads to the conclusion that ethane activation is the rate determining step for oxidising ethane and that the formation of the Wacker centre by water adsorption is rate determining for converting ethylene to acetic acid.

Key Words: **selective oxidation; kinetics; ethane; ethylene; acetic acid; mechanism.**

1. INTRODUCTION

Kinetics of the oxidation of ethane to acetic acid have been rarely studied; no comprehensive data are available. In the pioneering work of Thorsteinson *et al.* (1) the kinetics of ethane oxidation to acetic acid were investigated in a continuously stirred tank reactor for a catalyst of stoichiometry $Mo_1V_{0.25}Nb_{0.12}O_x$ in the temperature range from 548 to 598 K at elevated pressure of 2.07 MPa. A consecutive reaction with ethylene as an intermediate product to acetic acid was suggested. The formation of carbon monoxide and carbon dioxide was exclusively ascribed to the oxidation of ethylene. No evidence for carbon monoxide oxidation to carbon dioxide was found. The rate equations considered an inhibiting effect of ethylene and an acceleration by water on the rate of ethylene conversion to acetic acid. Apart from Thorsteinson's work no effort has been made to model the kinetics of ethane oxidation to acetic acid. Burch and Swarnakar (2) studied the oxidation of ethane to ethylene on a $Mo_1V_{0.5}Nb_{0.167}O_x$ catalyst but did not detect acetic acid under their reaction conditions (T: 643 ··· 683 K, P: 0.1 MPa). Their study focused on determining the orders of reaction which were 0.8 to 1 with respect to ethane and 0.07 to 0.5 with respect to oxygen depending on temperature.

Recently Borchert *et al.* showed that palladium doping of the above catalytic system leads to highly selective catalysts for acetic acid from ethane (3). For $Mo_1V_{0.25}Nb_{0.12}Pd_{0.0005}O_x$, which corresponds generally, apart from palladium, to the MoVnbO catalyst as studied by Thorsteinson *et al.*, highly improved selectivities to acetic acid were observed. At a temperature of 553 K and a total pressure of 1.5 MPa the selectivity to acetic acid amounted to 78% at an ethane conversion of 10% with palladium but only 32% at an ethane conversion of 9% without palladium (3).

The reaction scheme that we suggested (4) for the oxidation of ethane includes a parallel reaction to ethylene and to acetic acid as well as a consecutive reaction of the intermediate ethylene to acetic acid. Since the consecutive reaction is favoured at low temperature it is clear that the activation energy of the oxidation of ethane to ethylene must be lower than the activation energy of the direct oxidation of ethane to acetic acid. Carbon dioxide is formed from ethane, ethylene, and acetic acid. The role of water in this scheme can be summarised as follows: The rate of ethylene oxidation to acetic acid is strongly depending on the water partial pressure, which was derived from experiments with ethylene in the feed. There is also an influence of water on the rate of selective oxidation of ethane which

[1] To whom correspondence should be addressed. E-mail: baerns@aca-berlin.de. Fax: +49 30 6392-4454.

0021-9517/02 $35.00

was found to be small, however. We have explained the effect of water on the oxidation of ethylene to acetic acid in (4) by a Wacker-type mechanism; some aspects of this reaction need to be further explained. The heterogeneous analogue of the Wacker oxidation can be performed over redox catalysts like V_2O_5 or heteropoly acids doped with small amounts of palladium (5–8). As in the homogeneous Wacker reaction the presence of palladium in the catalyst is necessary to perform the heterogeneous Wacker oxidation effectively. One difference of the homogeneous reaction is that acetic acid is formed as main product instead of acetaldehyde with increasing temperature. For the influence of water in the heterogeneous Wacker oxidation power-law rate equations were reported, which describe its effect in a formal manner (9). No rate equations have been reported which are based on mechanistic considerations and account for the influence of water.

In the present study we report on kinetic models for the oxidation of ethane to acetic acid for the catalyst $Mo_1V_{0.25}Nb_{0.12}Pd_{0.0005}O_x$ (3). The aim was to kinetically describe the effect of operating conditions on the oxidation of ethane which were published in (4). Two kinetic models were suggested and discriminated; they both take into account surface processes such as catalyst reduction by ethane or ethylene and reoxidation by oxygen and surface hydroxylation, which are important steps in the reaction mechanism. The models differ in the way selective oxidation and total oxidation reaction steps are attributed to the two different catalytic centres considered.

2. KINETIC EXPERIMENTS

The experimental setup used for the kinetic experiments and catalyst preparation are described (4).

Measurement of kinetic data was performed in the temperature range from 503 to 576 K and a total pressure range between 1.3 and 2.8 MPa. The catalyst mass was varied between 1 and 13.7 g. The catalyst was diluted with particles of quartz of the same size ($m_{cat} : m_{quartz} = 1:2$) to achieve nearly isothermal operation ($\Delta T_{max} = 8$ K). Nitrogen was used as a balance gas. All kinetic experiments were carried out with catalyst particles taken from the same charge. Deactivation of the catalyst was not found during experimental runs (<50 h), which is in accordance with patent literature (3).

The BET-surface area of the catalyst amounted to 9.3 ± 0.2 m^2/g.

3. KINETIC MODELLING

3.1. General Procedure

The tubular reactor used for providing the integral kinetic data was modelled as an isothermally operating, pseudo-homogeneous, one-dimensional plug-flow reactor. The presence of external mass or temperature gradients between catalyst particle and gas phase and the presence of internal concentration gradients inside the particle were checked for by calculation. No influence was found using the correlation of Hougen and Watson (10) for external mass transfer or the criteria of Maers (11) for external heat transfer and for internal mass transfer. Thus, the pseudo-homogeneous reactor model is suitable.

Taking into account gas phase components as well as surface species, material balances were set up for both species: Assuming steady-state conditions for the reaction and the validity of the perfect gas law, the material balance for a differential mass of catalyst for the gas phase species i then is

$$\frac{dp_i}{d(m_{cat}/\dot{V}_{0,RTP})} = RT \sum_j \nu_{ij} r_j, \qquad [1]$$

where r_j denotes the rate of the jth reaction expressed per mass unit of catalyst and ν_{ij} are the stoichiometric coefficients. Since r_j, as given by the formulation of the kinetic model and a set of kinetic parameters, are mere functions of p_i for the isothermal reactor model, Eq. [1] constitutes a first-order differential equation system in the p_i. The derivation of expressions for r_j for the kinetic models is discussed below.

In steady-state operation the mass balance of a surface species k is

$$\frac{d\theta_{k,ct}}{d(m_{cat}/\dot{V}_{0,RTP})} = \frac{N_a}{N_z \cdot A_{BET} \cdot \rho_{cat}} \sum_j \nu_{kj} r_j = 0. \qquad [2]$$

The steady-state surface coverage $\theta_{k,ct}$ for each centre type ct resulted from the numerical solution of the set of nonlinear equations (Eq. [2]) and the balance of the normalised surface coverage θ_{k,M_i} of the oxide surface:

$$1 = \sum_k \theta_{k,ct}. \qquad [3]$$

As demonstrated further below, different active centres have to be considered to describe the experimental kinetic data adequately. Therefore, balance equations (Eq. [3]) of surface coverage were used for each type of centre ct. In order to derive the normalised surface coverage for every species the set of Eqs. [2] and [3] was solved analytically for each centre using the software package Maple V R.5 (12).

The system of differential Eq. [1] was integrated numerically over the modified contact time $m_{cat}/\dot{V}_0$ by a Gear algorithm (13). In the parameter estimation procedure this integration was repeatedly performed in each iteration step for every experiment. To find the maximum-likelihood estimates for the parameters of a kinetic model the sum of squared residuals for all n experiments with i components per experiment was minimised:

$$\sum_n \sum_i (\chi_{i,exp} - \chi_{i,sin})^2 \rightarrow \text{MIN}. \qquad [4]$$

The sum included molar fractions of the reaction products acetic acid, ethylene, and carbon dioxide.

The minimisation was performed applying a two-stage strategy. First a genetic algorithm (14) was used to find rough estimates for the kinetic parameters within a wide range. The resulting set of parameters from the genetic algorithm was then further optimised using a Nelder–Mead optimisation technique (15), which permits faster convergence near the optimum than the genetic algorithm.

For the determination of activation energies and adsorption enthalpies, data from all temperatures were used simultaneously, where the preexponential factors refer to the middle temperature of 539 K, which is helpful for achieving convergence (20).

3.2. Bases of the Kinetic Models

A suitable kinetic model for the catalytic oxidation of ethane to acetic acid on $Mo_1V_{0.25}Nb_{0.12}Pd_{0.0005}O_x$ must be able to explain the following key observations which have been described in detail in (4):

(a) The change in the reaction paths with temperature: While at low temperature, ethane is oxidised via ethylene as a gas phase intermediate to acetic acid; at high temperature, direct formation of acetic acid from ethane dominates and acetic acid and ethylene are mainly formed in parallel. Therefore, a kinetic model must include two reaction paths to acetic acid. One of them is dominating at low temperature and the other one at high temperature.

(b) The strong acceleration of the rate of the ethylene oxidation to acetic acid by the presence of water.

(c) The minor dependency of the ethane oxidation rate on water. Depending on the water partial pressure a maximum of the ethane oxidation rate must be described by the model.

Before describing both kinetic models in detail the features in common as well as the differences are briefly summarised:

Common to both models:

- Two catalytic redox centres are required for both models; kinetic models with a single centre only cannot explain the results. This is mainly due to the different influences of water on the oxidation of ethane and on the oxidation of ethylene on one hand, and the nearly constant rate of carbon dioxide formation regardless of the water-partial pressure, on the other hand. The rate of reoxidation is considered to be proportional to the oxygen partial pressure and concentration of free reduced centres (following the concept of Mars and Van Krevelen (16)).
- Since $Mo_1V_{0.25}Nb_{0.12}Pd_{0.0005}O_x$ shows properties which are typical for heterogeneous Wacker catalysts, such as the presence of palladium in low concentration, the ability to undergo redox cycles and the accelerating effect of water in ethylene oxidation, concepts known from literature for the heterogeneous Wacker oxidation are adopted to the present kinetic models. Hydroxyl centres formed by adsorption of water are considered to be the essential prerequisite for the conversion of ethylene to acetic acid.

Differences between both kinetic models:

- Selective oxidation reactions to ethylene and acetic acid as well as total oxidation are described differently: In model A oxidation of ethane to ethylene, formation of acetic acid from ethane via a surface intermediate and total oxidation is ascribed to one catalytic centre. The second centre exclusively catalyses the oxidation of ethylene to acetic acid via the Wacker mechanism. In contrast to that, model B assumes one centre for all selective reaction pathways, i.e., the oxidation of ethane to ethylene the direct formation of acetic acid from ethane via a surface intermediate and the oxidation of ethylene to acetic acid. The second centre accounts for all total oxidation reactions.
- The dependency of the ethane oxidation rate on water is considered in a different way. We do consider two explanations which are summarised by the two alternative reaction schemes described further below.

Based on a mechanistic formulation shown in the middle and lower part of Figs. 1 and 2, rate equations for each reaction of models A and B were derived (Tables 1 and 2). The objective of the formulation was to account for the experimental observations with a minimum number of reaction steps; i.e., we do not exclusively consider elementary steps in the formulation of the reactions. For a sequence of reaction steps one step is assumed to be rate determining; e.g., in reaction 9 (Table 1), which actually is a sequence of oxidation steps, the activation of ethane on $[OM_zO]$ sites is assumed to be the rate determining step. This means that this step determines the rate of carbon dioxide and water formation from ethane. Since the equilibrium of oxidation reactions is on the product side, reverse reactions were not considered. This assumption leads to a rate equation where the rate is proportional to the ethane partial pressure and the concentration of the $[OM_zO]$ centres. Adsorption and desorption reactions are formulated as elementary reactions. Langmuir adsorption is assumed; i.e., no activity distribution for adsorption sites is considered. The desorption rate constant is expressed by the ratio of the adsorption rate constant (k_i) and equilibrium constant (K_i). For catalyst reoxidation often two reaction steps are considered (17, 18); first reversible oxygen adsorption occurs and is followed by dissociation:

$$O_2 \rightarrow O_{2,ads} \qquad r_a = k_a \cdot p_{O2} \cdot \theta_{free} \qquad [i]$$

$$O_{2,ads} \rightarrow 2O_{lattice} \qquad r_b = k_b \cdot \theta_{O2} \cdot \theta_{free}. \qquad [ii]$$

Since pulse experiments had shown (4) that no weakly adsorbed oxygen is present on the catalysts, surface

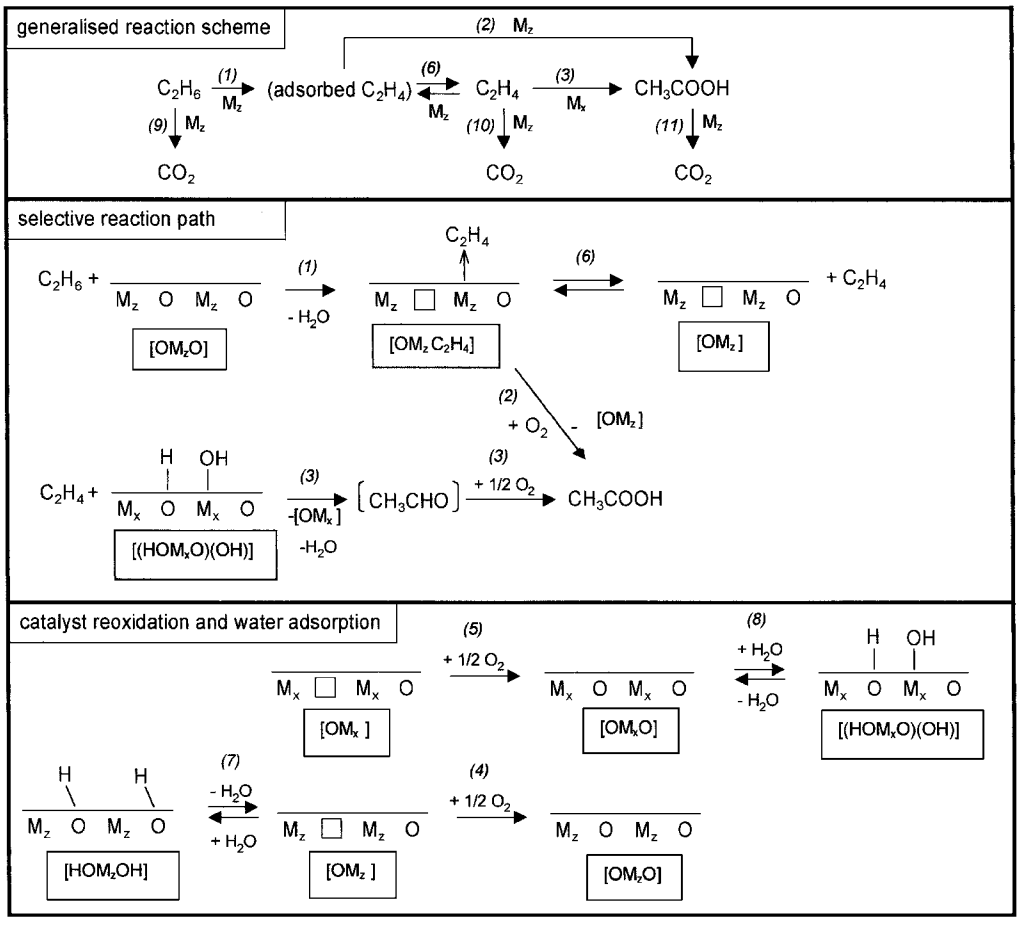

FIG. 1. Reaction scheme and mechanistic basis for reaction model A; numbers in parentheses assign the reaction to the rate equation's number in Table 1; oxygen vacancies are indicated with a square.

reaction [ii] must be much faster than reaction [i]. Thus the overall rate of reoxidation is given by a first-order rate equation as formulated in Table 1 (Eqs. [4] and [5]) and Table 2 (Eqs. [6] and [12]).

In the upper part of Figs. 1 and 2 the underlying reaction schemes of both models are shown. On each reaction arrow in the scheme the type of catalytic centre involved (e.g., M_z, M_x, or T) is specified and complemented by the index number used for the reactions in Tables 1 and 2. The abbreviations for the different states of the centres, e.g., $[OM_zO]$ or T–O for the oxidised form of centre M_z and T, which are used in the formulation of the rate equations (Tables 1 and 2), are shown in Figs. 1 and 2.

Model A (Fig. 1 and Table 1). The change in reaction pathway with temperature is described in model A by considering both a consecutive reaction of ethane to acetic acid with ethylene as gas phase intermediate (reactions 1, 3, 6) and a quasi-direct oxidation reaction of ethane to acetic acid via a surface intermediate (reactions 1, 2). For explaining the strong acceleration of the oxidation of ethylene to acetic acid by the presence of water vapour, it is assumed that the active form of the catalytic centre contains hydroxyl groups in analogy to the heterogeneous Wacker oxidation. By adsorption of water on the oxidised form $[OM_xO]$ of centre M_x, the active form for heterogeneous Wacker oxidation $[(HOM_xO)(OH)]$ is generated (reaction 8). Adsorption of water is therefore a prerequisite for oxidising ethylene to acetic acid. Since the concentration of the active form $[(HOM_xO)(OH)]$ of centre M_x increases with water partial pressure in the gas phase, the rate of the Wacker oxidation (reaction 3) increases as well with water partial pressure. A minor influence of water on ethane oxidation was found (4). Ethane conversion showed a weakly marked maximum with increasing water partial pressure. Model A considers this as follows. The centre M_z can convert ethane only in its oxidised form $[OM_zO]$. The reduced form $[OM_z]$ is inactive for ethane oxidation but can adsorb ethylene as well as water. Adsorption of ethylene (reaction 6) or water (reaction 7) on the reduced centre $[OM_z]$ leads to a blocking of centres. Therefore ethylene and water lead to a decrease in the concentration of reduced centres $[OM_z]$ as well as oxidised centres $[OM_zO]$. Since the rate of ethane oxidation is proportional to the concentration of $[OM_zO]$, the

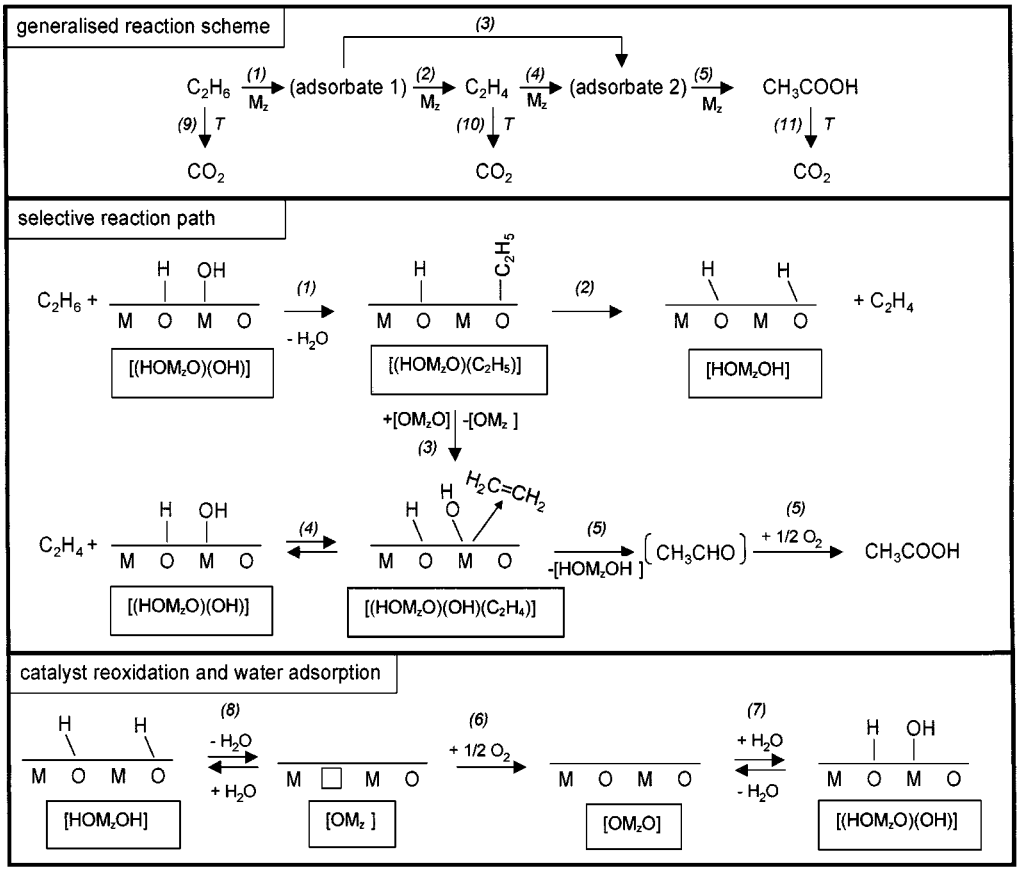

FIG. 2. Reaction scheme and mechanistic basis for reaction model B; numbers in parentheses assign the reaction to the rate equation's number in Table 2; oxygen vacancies are indicated with a square.

adsorption of ethylene or water lowers indirectly the rate of ethane oxidation. At low water partial pressure ethylene adsorption on the reduced centres should dominate, since the ethylene concentration has its maximum in that case. As a result of ethylene adsorption, the concentration of $[OM_zO]$ as well as the rate of ethane oxidation is decreased at low water partial pressure. On increasing the water partial pressure, the heterogeneous Wacker reaction on centre $[(HOM_xO)(OH)]$ is accelerated. Thus, the concentration of ethylene in the gas phase as well as on the reduced centre $[OM_z]$ decreases; thereby the rate of ethane oxidation increases. The adsorption of water on the reduced centre $[OM_z]$ is of importance only at high partial pressures of water. The $[HOM_zOH]$ species formed thereby are not reactive intermediates but occupy active centres. That is, the rate constant of water adsorption (k_7) is not kinetically relevant under steady-state conditions and is, therefore, not presented in Table 1. Nevertheless, the equilibrium constant K_7 has to be considered to describe the inhibition of ethane activation due to water adsorption.

The unselective oxidation reactions and the activation of ethane are ascribed to the catalytic centre type M_z. All three total oxidation reactions are initiated by the reaction of the oxidised form $[OM_zO]$ of M_z with the respective molecules (reactions 9–11).

Analytical expressions for calculating the normalised surface coverage of the adsorbates are given in the Appendix for model A.

Model B (Fig. 2 and Table 2). The mechanism for model B is shown in the middle and lower part of Fig. 2; the upper part shows the reaction scheme. The change in the reaction path found with increasing temperature is incorporated in model B similar to that in model A (see top part of Fig. 2). Again we consider both a consecutive reaction of ethane to acetic acid with ethylene as intermediate (reactions 1, 2, 4, 5) and a direct oxidation reaction of ethane to acetic acid (reactions 1, 3, 5). The two different catalytic centre types considered are centre type M_z for the selective oxidation reactions and centre type T for total oxidation (reactions 9–11). The background of assuming a centre exclusively for total oxidation is that certain undesirable phases (e.g., MoO_3) which cannot be completely avoided in the preparation of the catalyst may exclusively cause total oxidation. The reactions on the second catalytic redox centre T are not shown in Fig. 2. For centre T only two forms are considered

TABLE 1

Reactions, Rate Equations and Optimal Parameters for Model A

J	Reaction	Rate equation	Kinetic constant at 539 K	E_a or ΔH_{ads}
	Ethane activation (formation of adsorbed ethylene)			
1	$C_2H_6 + [OM_zO] \rightarrow [OM_zC_2H_4] + H_2O$	$r_1 = k_1 p_{C_2H_6} \theta_{[OM_zO]}$	$k_1 = 1.665 \cdot 10^{-9}$ mol (s kg Pa)$^{-1}$	99.7 kJ · mol^{-1}
	Acetic acid formation			
2	$[OM_zC_2H_4] + O_2 \rightarrow [OM_z] + CH_3COOH$	$r_2 = k_2 p_{O_2} \theta_{[OM_zC_2H_4]}$	$k_2 = 1.251 \cdot 10^{-9}$ mol (s kg Pa)$^{-1}$	92.6 kJ · mol^{-1}
3	$C_2H_4 + [(HOM_xO)(OH)] + 0.5\,O_2 \rightarrow CH_3COOH + [OM_x] + H_2O$	$r_3 = k_3 p_{C_2H_4} \theta_{[(HOM_xO)(OH)]}$	$k_3 = 1.254 \cdot 10^{-5}$ mol (s kg Pa)$^{-1}$	144 kJ · mol^{-1}
	Catalyst reoxidation			
4	$0.5\,O_2 + [OM_z] \rightarrow [OM_zO]$	$r_4 = k_4 p_{O_2} \theta_z$	$k_4 = 1.713 \cdot 10^{-8}$ mol (s kg Pa)$^{-1}$	123 kJ · mol^{-1}
5	$0.5\,O_2 + [OM_x] \rightarrow [OM_xO]$	$r_5 = k_5 p_{O_2} \theta_x$	$k_5 = 4.453 \cdot 10^{-9}$ mol (s kg Pa)$^{-1}$	85.2 kJ · mol^{-1}
	Ad-/ desorption of ethylene and water			
6	$C_2H_4 + [OM_z] \rightleftharpoons [OM_zC_2H_4]$	$r_6 = k_6 p_{C_2H_4} \theta_{[OM_z]} - k_6/K_6 \theta_{[OM_zC_2H_4]}$	$k_6 = 6.633 \cdot 10^{-8}$ mol (s kg Pa)$^{-1}$ $K_6 = 2.484 \cdot 10^{-4}$ Pa^{-1}	−137 kJ · mol^{-1} −176 kg · mol^{-1}
7	$H_2O + [OM_z] \rightleftharpoons [HOM_zOH]$	$r_7 = k_7 p_{H_2O} \theta_{[OM_z]} - k_7/K_7 \theta_{[HOM_zOH]}$	— $K_7 = 1.359 \cdot 10^{-7}$ Pa^{-1}	— −220 kJ · mol^{-1}
	Formation of Wacker-like centre			
8	$[OM_xO] + H_2O \rightleftharpoons [(HOM_xO)(OH)]$	$r_8 = k_8 p_{H_2O} \theta_{[OM_xO]} - k_8/K_8 \theta_{[(HOM_xO)(OH)]}$	$k_8 = 2.634 \cdot 10^{-9}$ mol (s kg Pa)$^{-1}$ $K_8 = 5.396 \cdot 10^{-6}$ Pa^{-1}	−25.7 kJ · mol^{-1} −38.8 kJ · mol^{-1}
	Unselective reaction steps			
9	$C_2H_6 + [OM_zO] + 3\,O_2 \rightarrow [*] \rightarrow 2\,CO_2 + 3\,H_2O + [OM_Z]$	$r_9 = k_9 p_{C_2H_6} \theta_{[OM_zO]}$	$k_9 = 3.363 \cdot 10^{-10}$ mol (s kg Pa)$^{-1}$	123 kJ · mol^{-1}
10	$C_2H_4 + [OM_zO] + 2.5\,O_2 \rightarrow [*] \rightarrow 2\,CO_2 + 2\,H_2O + [OM_Z]$	$r_{10} = k_{10} p_{C_2H_4} \theta_{[OM_zO]}$	$k_{10} = 2.019 \cdot 10^{-8}$ mol (s kg Pa)$^{-1}$	43.3 kJ · mol^{-1}
11	$CH_3COOH + [OM_zO] + 1.5\,O_2 \rightarrow [*] \rightarrow 2CO_2 + 2\,H_2O + [OM_Z]$	$r_{11} = k_{11} p_{HO_{ac}} \theta_{[OM_zO]}$	$k_{11} = 2.892 \cdot 10^{-9}$ mol (s kg Pa)$^{-1}$	105 kJ · mol^{-1}

namely the reduced form T and T–O the oxidised form. All reactions considered in model B are listed in Table 2 together with the respective rate equations.

The main difference in model B compared to model A refers to the activation of ethane. In model B, we consider that the active form of the centre type M_z must have a hydroxyl group for the oxidation of ethane as well as for the oxidation of ethylene. In this way model B can describe the increase of the rate of ethane oxidation if water is increased. Since water also adsorbs on the reduced form $[OM_z]$ (reaction 8), a further increase of water partial pressures cannot increase the rate of ethane oxidation above a certain limit, since the water adsorption decreases the reoxidation rate of centre $[OM_z]$. The active hydroxylated form $[(HOM_zO)(OH)]$ of oxidised centre $[OM_zO]$ is formed by adsorption of water (reaction 7).

Two minor additional differences to model A have to be mentioned. First, an intermediate $[(HOM_zO)(OH)(C_2H_4)]$ in the heterogeneous Wacker oxidation is explicitly considered (reactions 3 and 5) and second, ethylene adsorption

TABLE 2

Reactions and Rate Equations for Model B

j	Reaction	Rate equation
	Reactions on selective centre type M_z	
1	$C_2H_6 + [(HOM_zO)(OH)] \rightarrow -[(HOM_zO)(C_2H_5)] + H_2O$	$r_1 = k_1\, p_{C_2H_6} \theta_{[(HOM_zO)(OH)]}$
2	$[(HOM_zO)(C_2H_5)] \rightarrow C_2H_4 + [HOM_zOH]$	$r_2 = k_2 \theta_{[(HOM_zO)(C_2H_5)]}$
3	$[(HOM_zO)(C_2H_5)] + [OM_zO] \rightarrow [(HOM_zO)(OH)(C_2H_4)] + [OM_z]$	$r_3 = k_3 \theta_{[(HOM_zO)(C_2H_5)]}$
4	$C_2H_4 + [(HOM_zO)(OH)] \rightleftharpoons [(HOM_zO)(OH)(C_2H_4)]$	$r_4 = k_4\, p_{C_2H_4} \theta_{[(HOM_zO)(OH)]} - k_{r4} \theta_{[(HOM_zO)(OH)(C_2H_4)]}$
5	$[(HOM_zO)(OH)(C_2H_4)] + 0.5\,O_2 \rightarrow CH_3COOH + [HOM_zOH]$	$r_5 = k_5 \theta_{[(HOM_zO)(OH)(C_2H_4)]}$
6	$[OM_z] + 0.5\,O_2 \rightarrow [OM_zO]$	$r_6 = k_6\, p_{O_2} \theta_{[OM_z]}$
7	$[OM_zO] + H_2O \rightleftharpoons [(HOM_zO)(OH)]$	$r_7 = k_7\, p_{H_2O} \theta_{[OM_zO]} - k_{r7} \theta_{[(HOM_zO)(OH)]}$
8	$[HOM_zOH] \rightleftharpoons H_2O + [OM_z]$	$r_8 = k_8 \theta_{[HOM_zOH]} - k_{r_8}\, p_{H_2O} \theta_{[OM_z]}$
	Reactions on unselective centre type T	
9	$C_2H_6 + T - O + 3O_2 \rightarrow 2CO_2 + 3H_2O + T$	$r_9 = k_9\, p_{C_2H_4} \theta_{T-O}$
10	$C_2H_4 + T - O + 2.5O_2 \rightarrow 2CO_2 + 2H_2O + T$	$r_{10} = k_{10}\, p_{C_2H_4} \theta_{T-O}$
11	$CH_3COOH + T - O + 1.5O_2 \rightarrow 2CO_2 + 2H_2O + T$	$r_{11} = k_{11}\, p_{HO_{ac}} \theta_{T-O}$
12	$T + 0.5O_2 \rightarrow T - O$	$r_{12} = k_{12}\, p_{O_2} \theta_T$

TABLE 3

Experimental Conditions Used in Kinetic Experiments

P_{tot} (MPa)	Partial pressure $p_{i,e}$/kPa C_2H_6	O_2	H_2O	Temperature (K)	m_{cat} (g)	Flow rate (ml_{STP}/s)
Variation of space–time up to complete oxygen conversion						
1.30	650	130	0	503; 539; 576	1.0···13.7	1.5···11
1.40	646	129	108	503; 539; 576	1.0···13.7	1.5···11
1.60	640	128	320	503; 539; 576	1.0···13.7	1.5···11
Variation of partial pressures, low oxygen conversion						
1.60	320	128	0; 108; 320	503; 539; 576	2.0	2.5···5.1
1.60	640	128	0; 108; 320	503; 539; 576	2.0	2.5···5.1
1.60	640	192	0; 108; 320	503; 539; 576	2.0	2.5
Experiments at higher ethane partial pressure						
2.40	1100	120	300	503; 539	6.0; 13.7	6.0
2.40	1100	200	300	503; 539	6.0; 13.7	6.0
2.80	1250	120	300	539	4.0	4.0; 8.0

on the reduced form of centre $[OM_z]$ is disregarded. Taking ethylene adsorption into account had been a prerequisite of model A to explain the dependency of ethane oxidation rate from water concentration, which is explained here in a different way.

3.3. Data Basis

The following parameter range was covered by the kinetic experiments: $500 < T/K < 580$, $320 < p_{C_2H_6,inlet}/kPa < 1250$, $120 < p_{O_2,inlet}/kPa < 200$, $0 < p_{H_2O,inlet}/kPa < 320$.

The experimental conditions are listed in Table 3. Three groups of experiments can be distinguished:

(i) Experiments at varying space times at three temperatures ($T = 503$, 539, and 576 K) and three different water partial pressures at the reactor inlet ($p_{H_2O,in} = 0$, 108, 320 kPa).

(ii) Experiments at varying inlet partial pressures of oxygen and ethane. Again three temperatures ($T = 503$, 539, and 576 K) and three water inlet partial pressures ($p_{H_2O,in} = 0$, 108, 320 kPa) were studied. The oxygen conversion was kept small (at 503 and 539 K below $X_{O_2} = 15\%$, at $T = 576$ K below $X_{O_2} = 50\%$).

(iii) Experiments at high ethane partial pressures and incomplete oxygen conversion ($X_{O_2} < 90\%$). In contrast to the other experiments the water partial pressure was not varied and only two temperatures were studied.

The trace products (acetaldehyde, ethyl acetate, acetone, methanol, methane, propylene, ethanol) corresponding to an overall selectivity below 1% were not accounted for in kinetic modelling due to their low concentration.

4. RESULTS

From the variance estimates, defined as the sum of squared residuals for the maximum likelihood estimates of the kinetic parameters divided by degrees of freedom, it can be derived that model A is superior to model B (see Table 4). The well-known F test was applied to verify that model A is significantly better (19). The number of data N_d and the number of parameters N_p which are necessary to determine the degrees of freedom are given in Table 4. A confidence level of 99% was chosen for the F test. At this confidence level model A is significantly better, if $s^2(B)/s^2(A)$ is greater than 1.21/1.16/1.20 at $T = 503$, 539, and 576 K, respectively (see Table 4, right column). As this is the case for each temperature level, model A is significantly better than model B.

This finding is supported by the comparison of experimental and calculated molar fractions of the products as a function of space–time for both models shown in Fig. 3. The results of the fitting procedure for both models are compared with each other at three different temperature levels and three different water concentrations in the feed. Obviously model B does not appropriately describe the formation and conversion of ethylene as a reaction intermediate, which dominates at low temperature ($T = 503$ K). Without water added to the feed, model B did not describe the maximum in the ethylene concentration at a modified space–time of ca. 2×10^4 kg · s · m^{-3} in contrast to model A. With water in the feed both models gave fits of good quality across the whole temperature range studied (503 to 576 K). However, model B failed also in describing the apparent shift in the reaction path, which was found with increasing temperature in the experiments without water in the feed.

TABLE 4

Comparison of Variance Estimates s^2 for Models A and B at Different Temperatures

Data set	Model A $s^2(A)$	N_p	Model B $s^2(B)$	N_p	$s^2(B)/s^2(A)$
$T = 503$ K($N_d = 72$)	$8.395 \cdot 10^{-8}$	13	$2.342 \cdot 10^{-7}$	15	2.79
$T = 539$ K($N_d = 87$)	$6.799 \cdot 10^{-7}$	13	$1.436 \cdot 10^{-6}$	15	2.11
$T = 576$ K($N_d = 75$)	$3.858 \cdot 10^{-6}$	13	$9.884 \cdot 10^{-6}$	15	2.87

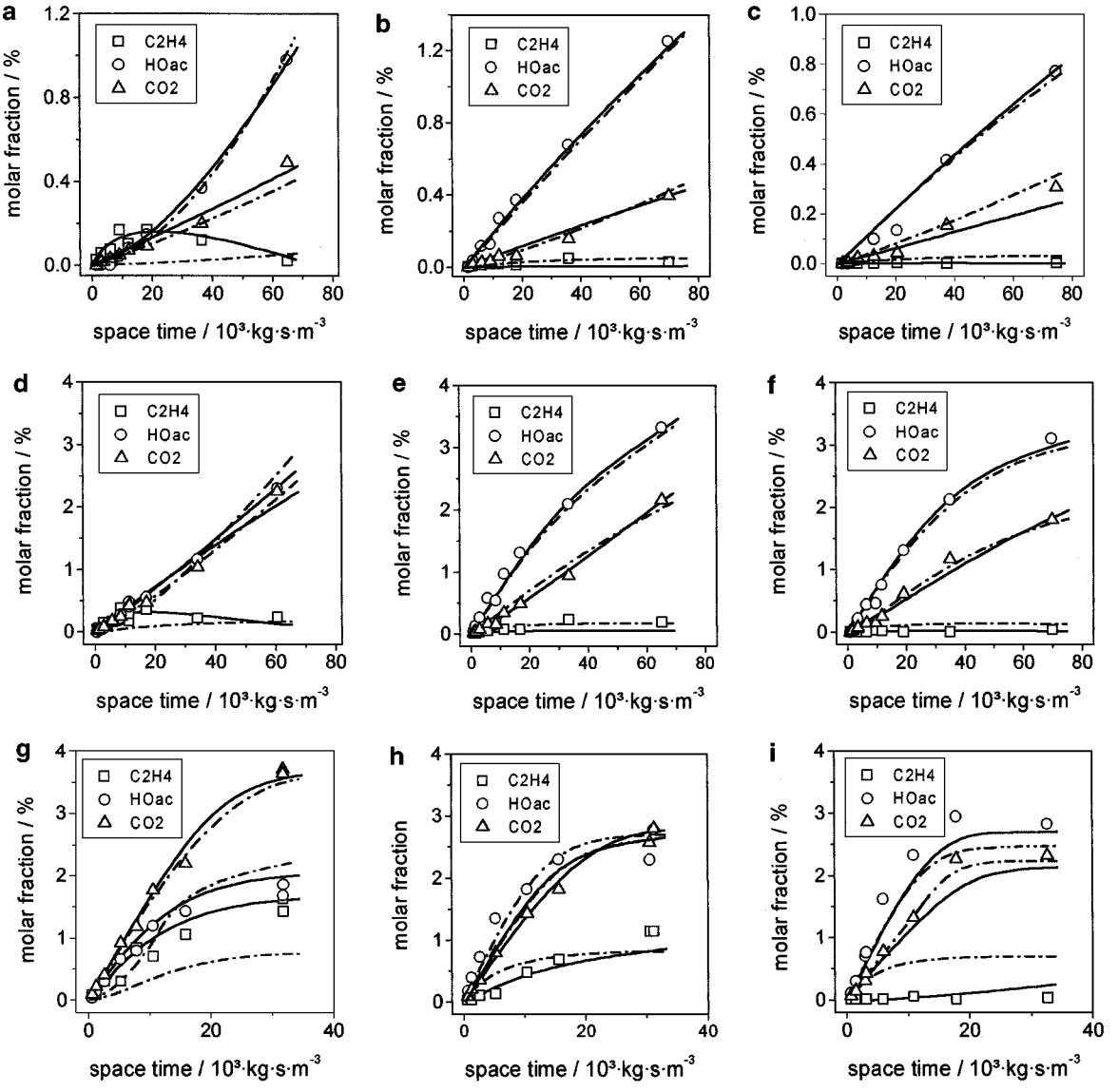

FIG. 3. Comparison of predicted and measured for molar fractions of products as function of space–time for model A (continuous lines) and model B (dashed lines) ($P_{tot} = 1.3/1.4/1.6$ MPa for $p_{H_2O,in} = 0/108/320$ kPa; $p_{C_2H_6,in} = 640 \ldots 650$ kPa; $p_{O_2,in} = 128 \ldots 130$ kPa), from left to right: $p_{H_2O;in} = 0/108/320$ kPa; (a)–(c) at $T = 503$ K, (d)–(f) at $T = 539$ K and (g)–(i) at $T = 576$ K.

Only model A could satisfactorily describe this shift in the reaction path with increasing temperature from mainly consecutive reaction of ethane via ethylene to acetic acid favoured at low temperature ($T = 503$ K) to mainly parallel formation of ethylene and acetic acid from ethane dominating at high temperature ($T = 576$ K). Thus, model A leads to an adequate description of the product formation in the range of conditions covered by the experiments. The optimal set of the kinetic parameters for the superior model A is given in Table 1 along with the respective reactions.

For the superior model A an additional comparison of experiment and simulation is shown in Fig. 4 for all data points included in the parameter estimation. The parity plots do not show systematic deviations. All points are equally spread around the diagonal line, which indicates that the error leading to the deviations is an experimental one but not model-based.

Since only model A can adequately describe the formation of all products in the range of experimental conditions studied (partial pressures of ethane, oxygen, water, residence time, and temperature), model B with its different mechanistic basis must be rejected. However, it must be emphasised that the successful application of model A does not prove that the underlying mechanistic assumptions are true, although they can be considered as reasonable.

5. DISCUSSION

For finding out which reaction is rate determining in the oxidation of ethane, the following reasoning is put

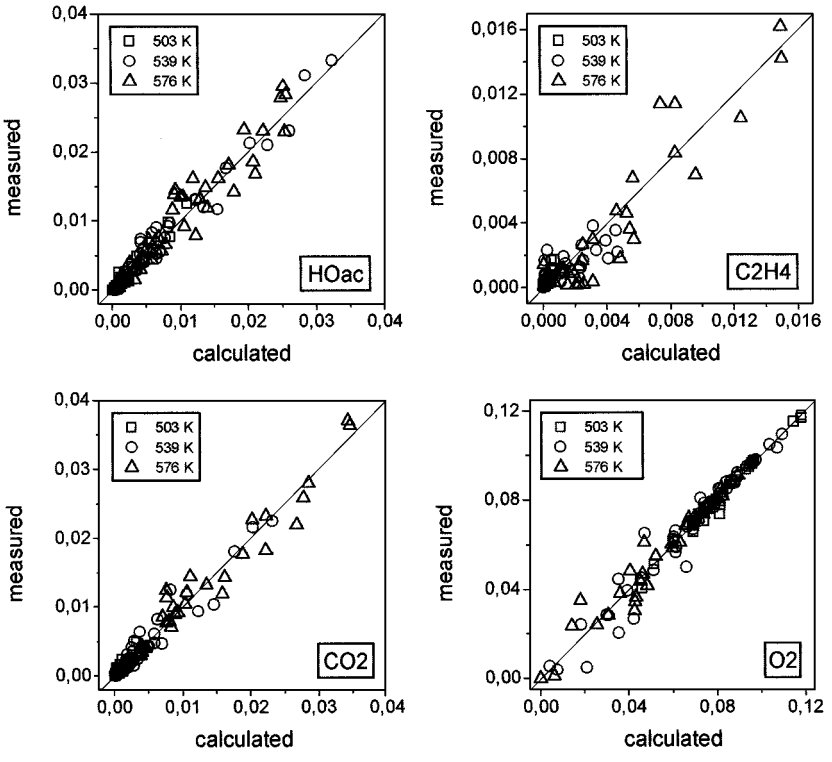

FIG. 4. Parity plots of measured and calculated molar fractions for model A including all data used in parameter estimation.

forward. It was discussed previously (4) that acetic acid desorption cannot be rate determining since different rates of acetic acid formation were found in ethylene and ethane oxidation. The results revealed as well that catalyst reoxidation is not rate determining; for illustration: in ethane oxidation the oxygen consumption is $4.3 \times 10^{-4}\,\mathrm{mol \cdot s^{-1} \cdot kg^{-1}}$ at $T = 539$ K, which is clearly below the value of $2.4 \times 10^{-3}\,\mathrm{mol \cdot s^{-1} \cdot kg^{-1}}$ found in ethylene oxidation at even lower temperature (520 K). Thus, it can be concluded that the activation of ethane is rate determining in the overall oxidation of ethane over $Mo_1V_{0.25}Nb_{0.12}Pd_{0.0005}O_x$.

Looking at the estimates for the parameters of the reactions 9, 10, 11 gives new insight into carbon dioxide formation. Since the reaction rates are calculated for the temperature $T = 539$ K it is evident that carbon dioxide originates approximately to the same extent from ethane, ethylene, and acetic acid for typical reaction conditions as applied in the experiments shown in Fig. 3. Due to the different activation energies of the total oxidation steps it can be seen that total oxidation of ethylene is the main origin of carbon dioxide at low temperature, while at high temperature total oxidation of ethane dominates.

Model A gives an indication about the role palladium plays in the reaction. As known from the literature the presence of palladium is necessary to perform an efficient, heterogeneous Wacker oxidation. Compared to the Pd-free analogue $Mo_1V_{0.25}Nb_{0.12}O_x$ the present catalyst showed much higher selectivity to acetic acid, typically around 80%, as compared to 26% reported by Thorsteinson *et al.* for the Pd-free catalyst (1). Thus we believe that the addition of palladium introduces catalytic activity for Wacker oxidation in the $Mo_1V_{0.25}Nb_{0.12}O_x$ catalytic system, which makes it possible to convert the ethylene formed effectively to acetic acid. In this way, the increase in acetic acid selectivity at the expense of ethylene selectivity is understandable. Borchert *et al.* (3) reported experimental results for Pd-free and Pd-containing $Mo_1V_{0.25}Nb_{0.12}O_x$ ($X_{C_2H_6} = 9\%$, respectively 10%), which showed that the rate of ethane oxidation is only slightly influenced by palladium. This underlines our argumentation that palladium mainly affects the oxidation of ethylene to acetic acid. According to kinetic model A the slight increase of ethane conversion can be as well attributed to the presence of palladium. Compared to the Pd-free catalyst the rate of ethane conversion is increased to a certain extent, since fast conversion of ethylene to acetic acid decreases the number of centres blocked by ethylene.

In the following part of the discussion we will analyse the confidence of kinetic model A. Since kinetic models are often nonlinear in their parameters, knowledge about the degree of nonlinearity present in the model should be gained. As an example for the analysis of nonlinear behaviour the conditional joint parameter likelihood regions (20) of model A were calculated. They are shown for certain confidence levels in Fig. 5. Wolf and Moros (14) have shown that plots of the conditional joint parameter likelihood regions of a kinetic model can be used to check if certain

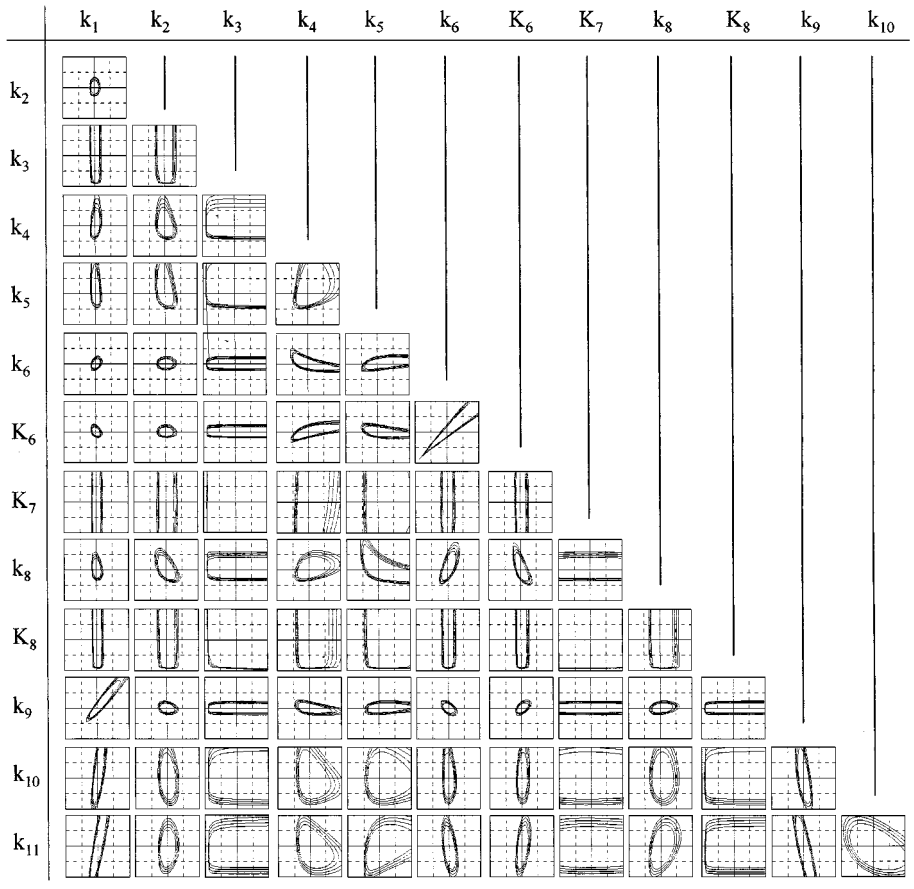

FIG. 5. Contour plots of the joint parameter likelihood regions for model A; the range of both kinetic parameters in each contour is between zero and two times the optimum value; the contours drawn stand for confidence levels of 99, 95, 80, and 50%.

reactions are fast compared to others, if the equilibrium of certain reactions is rapidly established, and if correlation between certain parameters exists.

For linear models the confidence regions have elliptical form. For model A we find the elliptical likelihood regions only for some parameter pairs (e.g., k_1/k_2, k_1/k_6, k_2/k_6, k_2/k_6, k_2/k_9, k_2/k_{10}, k_2/k_{11}). On the contrary in other plots strong deviations from the elliptical form appeared, indicating considerable nonlinearity in the kinetic model A. A typical joint parameter likelihood contour for linearly correlated parameters can be seen in the plot of the parameters k_6 and K_6. As a consequence all plots of k_6 and K_6 versus another parameter look similar. According to Wolf and Moros (14) the correlation of the adsorption rate constant k_6 and the equilibrium constant K_6 indicates that the equilibrium of the corresponding reaction, namely the adsorption of ethylene, is rapidly established. For parameter K_7 all contour plots show "valleys" which are open in both directions. Thus, it can be concluded that the corresponding reaction, the adsorption of water on reduced centres [OM_z] in model A, is of low significance at our experimental conditions. If all contours of a certain parameter show "valleys" which are closed in the direction of low parameter values but open to high values, it can be concluded that the reaction which belongs to this parameter is not rate determining, because the rate constant must be reduced strongly until a significant change in the results of the model prediction becomes obvious. This was found for k_3 and K_8. The contour plots of k_3 indicate that the heterogeneous Wacker oxidation (reaction 3) should be fast compared to the formation of the active form [$(HOM_xO)(OH)$] of the Wacker centre [OM_xO] (reaction 8). Contour plots of K_8 show that the desorption rate of water from the centre [OM_xO] (reaction 8), which is given as ratio k_8/K_8, is so slow compared to the adsorption reaction that desorption is not relevant. For the formation of carbon dioxide, the kinetic parameter for the oxidation of ethane has the smallest likelihood regions of all total oxidation reaction rate constants (Fig. 5). The wider likelihood regions of the kinetic constants belonging to the total oxidation of ethylene and acetic acid indicate that the values of their parameters are less significant.

The physico-chemical sense of the kinetic parameters of model A given in Table 1 is discussed in the following. In accordance with Van't Hoff's law negative values for the adsorption enthalpies were found (reactions 6–8). Furthermore, values of activation energies of reactions 1–5 and 9–

11 are positive as expected. However, for the rate constant k_6 of ethylene adsorption on the reduced centre $[OM_z]$ a highly negative activation energy is found. As indicated by the sensitivity analysis discussed above the parameters k_6 and K_6 of model A are highly correlated (Fig. 5). Thus, the activation energy of k_6 and adsorption enthalpy of K_6 cannot be determined independently from each other. Due to the correlation of the parameters only the quotient of k_6/K_6 is significant and therefore just the difference between the respective parameters $E_{a,k_6} - \Delta H_{ad,k_6} = 39\,\mathrm{kJ}\cdot\mathrm{mol}^{-1}$ can be determined. This corresponds to the activation energy of desorption; since this is positive its value is reasonable. For the activation energy of the rate constant for the formation of the Wacker-like centre $[(HOM_xO)(OH)]$, which is the active form (reaction 8), a small negative value was found as well. Here the sensitivity analysis led to the conclusion that no significant value for the rate of reverse reaction (water desorption) can be determined since the conversion of the Wacker centres via reaction 3 is much faster. Thus, actually reverse reaction 8 does not occur as long as ethylene is available for conversion of the $[(HOM_xO)(OH)]$ centres. The formation of Wacker centres is, however, a determining step for acetic acid formation. Thus, the negative value of activation energy is significant. From a mechanistic point of view, this could be explained by a decreasing number of Wacker sites with increasing temperature due to changes in the physical state of the catalyst (phase reconstruction, etc.). Indeed there are indications from differential scanning calorimetry experiments that a reversible transformation occurs at a temperature of approximately 550 K.

6. CONCLUSIONS

Two kinetic models for the catalytic ethane oxidation on the catalyst $Mo_1V_{0.25}Nb_{0.12}Pd_{0.0005}O_x$ to acetic acid were derived based on mechanistic considerations and the experimental results (4). The kinetic models include adsorbates as well as catalyst reduction and oxidation. According to the superior model A, ethane and ethylene are activated at different active centres. Strong adsorption of ethylene takes place at the centre for ethane activation. Consecutive conversion of ethylene at a second centre occurs via a heterogeneous Wacker oxidation mechanism which is related to hydroxyl groups forming the active centre. Hence, formation of acetic acid from ethylene can be accelerated to a certain degree due to the presence of water. Furthermore, the kinetic model describes the change in reaction pathway of consecutive formation of acetic acid from ethylene at low temperature to parallel formation of ethylene and acetic acid at high temperature.

The analysis of the results led to the conclusion that ethane activation is the rate determining step for oxidising ethane and that the formation of the centre for heterogeneous Wacker by means of water adsorption is rate determining for converting ethylene to acetic acid.

Since our kinetic model includes the influence of water partial pressure it can be used to optimise the amount of water used in a chemical process. This is of special interest since water on the one hand increases selectivity but on the other hand causes higher costs in concentrating the more diluted acetic acid. There clearly exists an optimum for the amount of water in a process. A study concerning operation and optimisation of fixed- and fluidised-bed reactors for the oxidation of ethane to acetic acid is presented in (Linke, D., Wolf, D., Baerns, M., Zeyβ, S., Dingerdissen, U., and Mleczko, L., *Chem. Eng. Sci.*, in press).

APPENDIX

The solution of equations for normalised coverage of adsorbates for superior model A follows.

$$\begin{aligned}
\theta_{[(HOM_xO)(OH)]} &= k_8 p_{O_2} p_{H_2O} \big/ \big(k_3 p_{O_2} p_{C_2H_4} + k_8 p_{O_2} p_{H_2O} \\
&\quad + k_3 k_8 \big/ K_5 p_{C_2H_4} p_{H_2O} + k_8 \big/ K_8 p_{O_2}\big).\\
\theta_{[OM_xO]} &= \big(k_3 p_{C_2H_4} + k_8/K_8\big) p_{O_2} \big/ \big(k_3 p_{O_2} p_{C_2H_4} \\
&\quad + k_8 p_{O_2} p_{H_2O} + k_3 k_8 \big/ k_5 p_{C_2H_4} p_{H_2O} \\
&\quad + k_8 \big/ K_8 p_{O_2}\big).\\
\theta_{[OM_x]} &= 1 - \theta_{[(HOM_xO)(OH)]} - \theta_{[OM_xO]}.\\
\theta_{[OM_ZO]} &= k_4 p_{O_2} \big(k_2 K_6 p_{O_2} + k_6\big) \big/ \big[\big(k_2 K_6 p_{O_2} + k_6\big) \\
&\quad \times \big(k_1 p_{C_2H_6} + k_9 p_{C_2H_6} + k_{10} p_{C_2H_4} \\
&\quad + k_{11} p_{HOac}\big) + K_7 p_{H_2O} \big(k_2 K_6 k_1 p_{C_2H_6} p_{O_2} \\
&\quad + k_2 K_6 k_9 p_{C_2H_6} p_{O_2} + k_2 K_6 k_{10} p_{O_2} p_{C_2H_4} \\
&\quad + k_2 K_6 k_{11} p_{O_2} p_{HOac} + k_6 k_1 p_{O_2H_6} \\
&\quad + k_6 k_9 p_{C_2H_6} + k_6 k_{10} p_{C_2H_4} + k_6 k_{11} p_{HOac}\big) \\
&\quad + K_6 \big(k_4 k_1 p_{C_2H_6} p_{O_2} + k_6 k_1 p_{C_2H_6} p_{C_2H_4} \\
&\quad + k_6 k_9 p_{C_2H_6} p_{C_2H_4} + k_6 k_{10} \big(p_{C_2H_4}\big)^2 \\
&\quad + k_6 k_{11} p_{C_2H_4} p_{HOac}\big) + k_4 p_{O_2} \big(k_2 k_6 p_{O_2} \\
&\quad + k_6\big)\big].\\
\theta_{[OM_ZC_2H_4]} &= K_6 \big(k_4 k_1 p_{C_2H_6} p_{O_2} + k_6 k_1 p_{C_2H_6} p_{C_2H_4} \\
&\quad + k_6 k_9 p_{C_2H_6} p_{C_2H_4} + k_6 k_{10} \big(p_{C_2H_4}\big)^2 \\
&\quad + k_6 k_{11} p_{C_2H_4} p_{HOac}\big) \big/ \big[\big(k_2 K_6 p_{O_2} + k_6\big) \\
&\quad \times \big(k_1 p_{C_2H_6} + k_9 p_{C_2H_6} + k_{10} p_{C_2H_4} + k_{11} p_{HOac}\big) \\
&\quad + K_7 p_{H_2O} \big(k_2 K_6 k_1 p_{C_2H_6} p_{O_2} + k_2 K_6 k_9 p_{O_2H_6} p_{O_2} \\
&\quad + k_2 K_6 k_{10} p_{O_2} p_{C_2H_4} + k_2 K_6 k_{11} p_{O_2} p_{HOac} \\
&\quad + k_6 k_1 p_{C_2H_6} + k_6 k_9 p_{C_2H_6} + k_6 k_{10} p_{C_2H_4} \\
&\quad + k_6 k_{11} p_{HOac}\big) + K_6 \big(k_4 k_1 p_{C_2H_6} p_{O_2} \\
&\quad + k_6 k_1 p_{C_2H_6} p_{C_2H_4} + k_6 k_9 p_{C_2H_6} p_{C_2H_4} \\
&\quad + k_6 k_{10} \big(p_{C_2H_4}\big)^2 + k_6 k_{11} p_{C_2H_4} p_{HOac}\big) \\
&\quad + k_4 p_{O_2} \big(k_2 K_6 p_{O_2} + k_6\big)\big].
\end{aligned}$$

$$\theta_{[HOM_ZOH]} = K_7 p_{H_2O}\left(k_2k_6k_1 p_{C_2H_6} p_{O_2} + k_2K_6k_9 p_{C_2H_6} p_{O_2} + k_2K_6k_{10} p_{O_2} p_{C_2H_4} + k_2K_6k_{11} p_{O_2} p_{HOac} + k_6k_1 p_{C_2H_6} + k_6k_9 p_{C_2H_6} + k_6k_{10} p_{C_2H_4} + k_6k_{11} p_{HOac}\right) / \left[\left(k_2K_6 p_{O_2} + k_6\right)\left(k_1 p_{C_2H_6} + k_9 p_{C_2H_6} + k_{10} p_{C_2H_4} + k_{11} p_{HOac}\right) + K_7 p_{H_2O}\left(k_2K_6k_1 p_{C_2H_6} p_{O_2} + k_2K_6k_9 p_{C_2H_6} p_{O_2} + k_2K_6k_{10} p_{O_2} p_{C_2H_4} + k_2K_6k_{11} p_{O_2} p_{HOac} + k_6k_1 p_{C_2H_6} + k_6k_9 p_{C_2H_6} + k_6k_{10} p_{C_2H_4} + k_6k_{11} p_{HOac}\right) + K_6(k_4k_1 p_{C_2H_6} p_{O_2} + k_6k_1 p_{C_2H_6} p_{C_2H_4} + k_6k_9 p_{C_2H_6} p_{C_2H_4} + k_6k_{10}\left(p_{C_2H_4}\right)^2 + k_6k_{11} p_{C_2H_6} p_{HOac}\right) + k_4 p_{O_2}\left(k_2K_6 p_{O_2} + k_6\right)\right].$$

$$\theta_{[OM_Z]} = 1 - \theta_{[OM_ZO]} - \theta_{[OM_ZC_2H_4]} - \theta_{[HOM_ZOH]}.$$

APPENDIX: NOTATION

Symbols

A_{BET}	surface area per mass of catalyst determined by BET method ($m^2 \cdot kg^{-1}$)
ac	acetyl group (–CO–CH_3)
E_a	activation energy (kJ mol^{-1})
k	rate constant (mol kg^{-1} s^{-1} Pa^x)
K	equilibrium constant (pa^x)
m_{cat}	mass of catalyst (kg)
N_a	Avogadro number (mol^{-1})
N_d	number of independent data points (number of experiments × number of independent components)
N_p	number of model parameters
N_z	density of active centres of type M_z on the catalyst surface (m^{-2})
P	total pressure (Pa)
p	partial pressure (Pa)
r	rate of a single reaction (mol kg^{-1} s^{-1})
s^z	variance
R	gas constant (J K^{-1} mol^{-1})
T	temperature (K)
$\dot{V}_0$	total flow rate of reactor inlet (m^3 s^{-1})

Greek Symbols

χ	molar fraction
θ	surface coverage normalised with the number of centres of the same type
ρ_{cat}	density of catalyst bed (kg m^{-3})
τ	modified space time, defined as catalyst mass divided by volumetric flow
υ	stoichiometric coefficient

Subscripts

exp	experimental value
i	ith gas phase component
j	jth reaction
k	kth species on catalyst surface
mod	modelled value obtained by numerical calculations
RTP	reaction temperature and pressure (for volumes)
STP	standard temperature and pressure (for volumes)
z	type of catalytic centre

REFERENCES

1. Thorsteinson, E. M., Wilson, T. P., Young, F. G., and Kasai, P. H., *J. Catal.* **52**, 116 (1978).
2. Burch, R., and Swarnakar, R., *Appl. Catal.* **70**, 129 (1991).
3. Borchert, H., and Dingerdissen, U. (Hoechst), Ger. Offen. DE 19 630 832, 1998.
4. Linke, D., Wolf, D., Baerns, M., Dingerdissen, U., and Zeyß, S., *J. Catal.*, doi: 10,1006/jcat. 2001. 3367.
5. Evnin, A. B., Rabo, J. A., and Kasai, P. H., *J. Catal.* **30**, 109 (1973).
6. Seoane, J. L., Boutry, P., and Montarnal, R., *J. Catal.* **63**, 191 (1980).
7. Van der Heide, E., De Wind, M., Gerritsen, A. W., and Scholten, J. J. F., "Proceedings, 9th International Congress on Catalysis, Calgary, 1988" (M. J. Phillips and M. Ternan, Eds.), p. 1648. Chem. Institute of Canada, Ottawa, 1988.
8. Nowinska, K., and Dudko, D., *Appl. Catal. A* **159**, 75 (1997).
9. Forni, L., and Terzoni, G., *Ind. Eng. Chem. Process. Res. Dev.* **16**, 288 (1977).
10. Hougen, O. A., and Watson, K. M., "Chemical Process Principals," Part III. Wiley, New York, 1947.
11. Maers, D. E., *J. Catal.* **20**, 127 (1971); Maers, D. E., *Ind Eng. Chem. Proc. Des. Dev.* **10**, 541 (1971).
12. Monagan M. B., Geddes, K. O., Heal, K. M., Labahn, G., and Vorkoetter, S. M., "Maple V—Programming Guide." Springer-Verlag, New York, 1998.
13. Gear, C. W., "Numerical Initial Value Problems in Ordinary Differential Equations." Prentice-Hall International, Englewood Cliffs, NJ, 1971.
14. Wolf, D., and Moros, R., *Chem. Eng. Sci.* **52**, 1189 (1997).
15. Nelder, J. A., and Maed, R., *Comp. J.* **7**, 308 (1965).
16. Mars, P., and Van Krevelen, D. W., *Chem. Eng. Sci.* **3**, 41 (1954).
17. Kondratenko, E. V., Buyevskaya, O. V., Soick, M., and Baerns, M., *Catal. Lett.* **63**, 153 (1999).
18. Freund, F., Maiti, G. C., Batllo, F., and Baerns, M., *J. Chem. Phys.* **87**, 1467 (1990).
19. Schoemaker, D. P., Garland, C. W., and Nibler, J. W., *in* "Experiments in Physical Chemistry," 5th ed., p. 815. McGraw–Hill, New York, 1989.
20. Bates, D. M., and Watts, D. G., "Nonlinear Regression Analysis and Its Applications." Wiley, New York, 1988.